Author's personal copy

Journal of Quantitative Spectroscopy & Radiative Transfer 112 (2011) 2310–2322

Contents lists available at ScienceDirect

Journal of Quantitative Spectroscopy & Radiative Transfer

journal homepage: www.elsevier.com/locate/jqsrt

Revision of spectral parameters for the B- and γ-bands of oxygen and their validation against atmospheric spectra

Iouli E. Gordon [a,*], Laurence S. Rothman [a], Geoffrey C. Toon [b]

[a] Harvard-Smithsonian Center for Astrophysics, Atomic and Molecular Physics Division, Cambridge, MA 02138, USA
[b] Jet Propulsion Laboratory, California Institute of Technology, Pasadena, CA 91109, USA

ARTICLE INFO

Article history:
Received 25 March 2011
Received in revised form
16 May 2011
Accepted 17 May 2011
Available online 25 May 2011

Keywords:
HITRAN
Oxygen spectroscopy
B-band
γ-Band

ABSTRACT

Until recently the B ($b^1\Sigma_g^+$ ($v=1$)–$X^3\Sigma_g^-$ ($v=0$)) and γ ($b^1\Sigma_g^+$ ($v=2$)–$X^3\Sigma_g^-$ ($v=0$)) bands of oxygen in the visible region had not been used extensively in satellite remote sensing of the atmosphere. These bands roughly cover the regions around 14,527 and 15,904 cm^{-1}, respectively (0.69 and 0.63 μm). However, these bands (in particular the B-band) are now being increasingly considered for future satellite missions. In this light, it is important to make sure that the reference spectroscopic parameters allow accurate retrieval of important physical characteristics from the atmospheric spectra. The spectroscopic parameters currently given for these bands in the HITRAN2008 spectroscopic database were tested against high-resolution atmospheric spectra measured with solar-pointing Fourier transform spectrometers at Park Falls, Wisconsin (B-band) and Kitt Peak, Arizona (γ-band). It was found that the current HITRAN parameters cannot produce satisfactory fits of the observed spectra. In order to improve the database we have collected the best available measured line positions that involve the $b^1\Sigma_g^+$ ($v=1$ and $v=2$) states for the three most abundant isotopologues of oxygen and performed a combined fit to obtain a consistent set of spectroscopic constants. These constants were then used to calculate the line positions. A careful review of the available intensity and line-shape measurements was also carried out, and new parameters were derived based on that review. In particular, line shift parameters, that were not previously available, were introduced. The new data have been validated using the high-resolution atmospheric spectra measured with the Fourier transform spectrometers at Park Falls, Wisconsin (B-band) and Kitt Peak, Arizona (γ-band) and have yielded substantial improvement. In addition, we report the first direct observation and analysis of the $^{16}O^{18}O$ lines in the γ-band.

© 2011 Elsevier Ltd. All rights reserved.

1. Introduction

1.1. Motivation

The atmospheric dry mole fraction of O_2 is highly constant (0.2094). Thus, in atmospheric remote sensing, O_2 absorption lines allow an accurate determination of the atmospheric air mass traversed by the measured photons. This can reduce errors due to air-mass uncertainties in simultaneous measurements of other gases of scientific interest (e.g., CO_2, CH_4). Provision for simultaneous measurement of O_2, along with the atmospheric gases of interest, for air-mass calibration purposes, is now commonplace in near-IR remote sensors (e.g., Orbiting Carbon Observatory (OCO) [1], Greenhouse gases Observing SATellite (GOSAT) [2], and SCanning Imaging Absorption spectroMeter for Atmospheric CHartographY (SCIAMACHY) [3]).

Air-mass calibration is particularly important for space-borne measurements of reflected sunlight. In this observation geometry clouds and aerosol can significantly perturb

* Corresponding author: Tel.: +1 617 496 2259.
E-mail address: igordon@cfa.harvard.edu (I.E. Gordon).

0022-4073/$ - see front matter © 2011 Elsevier Ltd. All rights reserved.
doi:10.1016/j.jqsrt.2011.05.007

Author's personal copy

the atmospheric path-length distribution. To date, the O_2 A-band at 760 nm has been the favorite choice for air-mass calibration, although Nowlan et al. [4] have assessed the potential of using the B-band as well in application to ACE-MAESTRO retrievals. There are significant advantages to additionally using the O_2 B-band, centered at 688 nm, despite its relatively strong overlap with water vapor lines. Firstly, the B-band lines are 15 times weaker than the A-band lines and are more similar in strength to those of the green house gases (GHG) of interest, minimizing the impacts of common systematic errors. Secondly, chlorophyll absorbs solar radiation in the 400–600 nm range and re-emits it at 660–780 nm. This so-called fluorescence emission is the most direct remote-sensing indicator of vegetation growth. Expressed as a fraction of the total reflected solar radiation, fluorescence emission peaks near 683 nm, where it can be as much as 5% of the total reflected solar flux. This compares with only ~1–2% in the A-band region. So for the purposes of accurately measuring chlorophyll emission from space, together with the GHGs that are exchanged during vegetation growth, the B-band region provides valuable additional information. Note that without correction for chlorophyll emission, the A-band will yield a biased O_2 column over actively growing vegetation [5].

Another application that employs the B-band is analysis of cloud-top height and cloud coverage [6,7]. Also individual rovibronic lines in the B-band are used for wind measurements above 20 km, while those from the γ-band are used for measurements below 20 km [8].

1.2. Status of the current HITRAN parameters

The construction of the current HITRAN line list for the oxygen B- and γ-bands was carried out by Gamache et al. [9] in 1998, with the exception of the air-broadened half widths that were updated in HITRAN2004 [10] based on the measurements of the oxygen A-band [11].

The line positions of the B-band for the principal isotopologue were calculated using ground-state constants from Rouillé et al. [12] and upper-state constants taken from Albritton et al. [13] who refitted the 1948 solar atmospheric spectrum of Babcock and Herzberg [14]. For the $^{16}O^{18}O$ and $^{16}O^{17}O$ species, unpublished constants for the upper state from Benedict and Brault (based on solar spectra recorded with the Fourier transform spectrometer at the Kitt Peak National Solar Observatory in 1982) were used. In the case of $^{16}O^{17}O$, the line positions as observed directly in the atmospheric spectrum by Benedict and Brault were used. No line shift parameters were assigned to the lines in the B-band [15]. The intensities for $^{16}O_2$ and $^{16}O^{18}O$ were based on the Einstein A-coefficient reported in the experimental work of Giver et al. [16], while for $^{16}O^{17}O$ they were based on a private communication with Benedict and Brault. The self-broadening parameters for all isotopologues were based on the Giver et al. [16] measurements.

The line positions in the γ-band for $^{16}O_2$ were calculated using the constants from Albritton et al. [13], while for $^{16}O^{18}O$ the isotopic scaling of the $^{16}O_2$ constants was used. The intensities and self-broadening coefficients were based on the work of Mélières et al. [17], while A-band values [11] were adapted for the air-broadening coefficients. No $^{16}O^{17}O$ lines were given in this band due to their low intensity. Similar to the B-band, no line shift parameters had been assigned to the lines in γ-band.

1.3. Atmospheric retrievals using HITRAN parameters

Fig. 1 shows a fit to a solar atmospheric spectrum recorded at the Total Column Carbon Observing Network (TCCON) site in Park Falls, Wisconsin, on December 22, 2004, at a solar zenith angle of 82.45°. The black points represent the measured spectrum. The black curve is the calculation. The colored lines represent the contributions to the calculated transmittance from the various gases/isotopologues. The red curve represents the $^{16}O_2$ isotopologue (denoted as "1o2" in the figure), the orange curve represents the $^{16}O^{18}O$ isotopologue (2o2), and the lime-green curve represents the $^{16}O^{17}O$ isotopologue (3o2). The green curve represents H_2O absorption, and the dark blue curve represents the solar (Fraunhofer) absorption lines. The "Residuals" represent the difference between the measured and calculated spectra.

At the time this spectrum was measured, the outside temperature was 250 K, resulting in a very small H_2O column, thus minimizing the visual impact of interfering H_2O lines. The top panel shows fits obtained using the HITRAN 2008 line list, while the bottom panel shows the fits obtained by replacing all oxygen lines with the new line list described in this work. As can be seen from the top panel, the use of HITRAN2008 spectral parameters [18] (which have not changed for the B-band from those derived in Ref. [9], with the exception of air-broadening coefficients) leads to large residuals in comparison with the observed spectrum. The main problems seem to arise from: (1) a rapidly growing (with increase of rotational quantum number) deviation of HITRAN line positions from the observed ones (up to 0.01 cm^{-1}) for all isotopologues, (2) absence of line shifts, and (3) significant overestimation of $^{16}O^{17}O$ intensities (see Section 2.2 for details). The discussion of the bottom panel is in the validation section of this paper.

Fig. 2 shows the solar atmospheric spectrum covering the O_2 γ-band recorded by the FTS at the McMath solar telescope, Kitt Peak, Arizona. (TCCON spectra do not cover this region). This spectrum was measured on June 19, 1983 at a solar zenith angle of 86.9°. The large lower-most panel shows a fit obtained using the new line list described in this work. The three narrow panels show the spectral residuals obtained from spectral fits using: (a) HITRAN 2008 (that remained practically unchanged from the HITRAN1996 edition [19]), (b) HITRAN 2008 supplemented by the two missing lines at the band head that regretfully had disappeared from the database starting from HITRAN2004 [10], and (c) the new line list described in this work. In (a), the residuals are completely dominated by the two strong missing $^{16}O_2$ lines at the band head at 15,927.5 cm^{-1}. These cause spectral residuals exceeding 90% in this particular spectrum. In (b) the residuals are much improved with the rms down to 0.672% and dominated by (i) neglect of line mixing at the band head, (ii) interfering H_2O absorptions at the

Author's personal copy

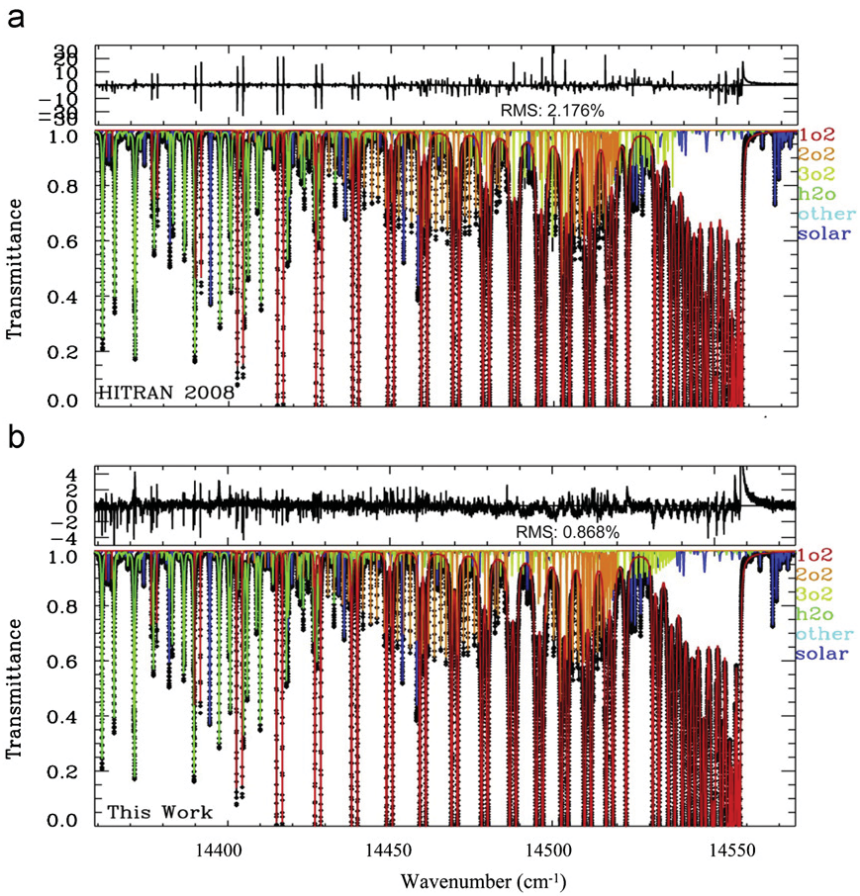

Fig. 1. Atmospheric spectrum (B-band region) recorded by the solar-pointing FTS in Park Falls, Wisconsin, on December 22, 2004. The large panels show a fit obtained using (a) HITRAN 2008 and (b) the new line list described in this work, while the smaller panels show the spectral residuals obtained from spectral fits. (For interpretation of the references to color in this figure legend, the reader is referred to the web version of this article.)

lower frequencies, and (iii) the poor quality of the $^{16}O^{18}O$ spectroscopy. In HITRAN 2008 only the strongest 22 lines of the $^{16}O^{18}O$ isotopologue were tabulated due to somewhat over-restricted minimum strength criterion, and these had position errors of up to 0.07 cm^{-1}. The residuals in panel (c) will be discussed in the validation section below.

In order to minimize the inaccuracies in spectral parameters listed above, all available laboratory spectroscopic information relevant to the B- and γ-band has been collected, critically evaluated, and used to construct a new line list (at the reference temperature of 296 K) described in this paper. The line lists have then been validated against atmospheric spectra from Park Falls and Kitt Peak.

2. B-band

2.1. Line positions

2.1.1. $^{16}O_2$

The line positions in the B-band were calculated using spectroscopic constants given in Table 1. For the principal isotopologue, these constants were obtained by global fitting of the microwave (MW), Raman, $b^1\Sigma_g^+$ $(v=1)-a^1\Delta_g$ $(v=0)$, $a^1\Delta_g$ $(v=0)-X^3\Sigma_g^-$ $(v=0)$, and $b^1\Sigma_g^+$ $(v=1)-X^3\Sigma_g^-$ $(v=0)$ data. The microwave data were taken from the supplementary material of Ref. [20] that contains the measurements carried out in that work and references therein. Measurements of Rouillé et al. [12] and Millot et al. [21] were used for the Raman data. The $b^1\Sigma_g^+$ $(v=1)-a^1\Delta_g$ $(v=0)$ transitions were taken from Ref. [22], while $a^1\Delta_g$ $(v=0)-X^3\Sigma_g^-$ $(v=0)$ transitions were from Ref. [23]. Line positions reported by Cheah et al. [24] and those provided to us by the authors of Ref. [25] were used for the $b^1\Sigma_g^+$ $(v=1)-X^3\Sigma_g^-$ $(v=0)$ data itself. Interestingly, the measurements of the line positions in the B-band by Cheah et al. [24] appear to be of significantly higher quality than the measurements of the $a^1\Delta_g$ $(v=0)-X^3\Sigma_g^-$ $(v=0)$ reported in the same paper. The line positions of the latter band in Cheah et al. [24] were found to be systematically off by 0.02 cm^{-1} [23]. In fact, the combined fit of $b^1\Sigma_g^+$ $(v=1)-X^3\Sigma_g^-$ $(v=0)$ and $a^1\Delta_g$ $(v=0)-X^3\Sigma_g^-$ $(v=0)$ bands from Cheah et al. [24], and $b^1\Sigma_g^+$ $(v=1)-a^1\Delta_g$ $(v=0)$ from Ref. [22] is of significantly inferior quality than when the data for $a^1\Delta_g$ $(v=0)-X^3\Sigma_g^-$ $(v=0)$ band is replaced with the one from Leshchishina et al. [23].

Regrettably, in the global fit performed here, the line positions in the B-band measured by Phillips et al. [26] could not be included as they are not provided in the

Author's personal copy

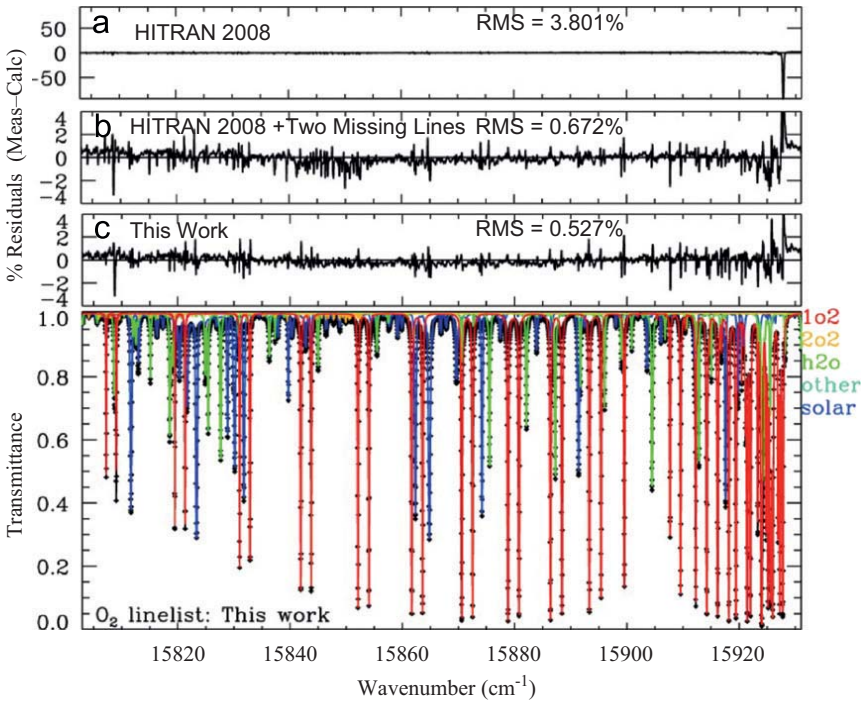

Fig. 2. Atmospheric spectrum (γ-band region) recorded by the solar-pointing FTS at the McMath solar telescope, Kitt Peak, Arizona. The large lower-most panel shows a fit obtained using the new line list described in this work. The three narrow panels show the spectral residuals obtained from spectral fits using: (a) HITRAN 2008, (b) HITRAN 2008 supplemented by the two missing lines at the band head, and (c) the new line list described in this work.

Table 1
Spectroscopic parameters of the $v=1$ and 2 levels of the $b^1\Sigma_g^+$ state of $^{16}O_2$.

Parameters (cm^{-1})	This work	Albritton et al. [13] [a]	Cheah et al. [24]	Phillips et al. [26]	Naus et al. [29]
T_1	14,526.9896(12)[b]	14,526.9909(17)	14,525.65553(26)	14,526.9976(12)[b]	
B_1	1.3729553(72)	1.372982(10)	1.3729659(22)	1.372951(18)	
D_1	$5.3960(93)\times10^{-6}$	$5.418(10)\times10^{-6}$	$5.4086(42)\times10^{-6}$	$5.397(50)\times10^{-6}$	
T_2	15,903.7479(27)[b]	15,903.7509(16)[b]	15,902.4251(32)		15,903.748(3)[b]
B_2	1.354630(23)	1.354609(11)	1.354644(38)		1.35463(2)
D_2	$5.484(36)\times10^{-6}$				
Number of lines used in this work per band	MW: 85; Raman: 94; $b^1\Sigma_g^+-a^1\Delta_g$: 29; $a^1\Delta_g-X^3\Sigma_g^-$: 199; $b^1\Sigma_g^+$ ($v=1$)$-X^3\Sigma_g^-$ ($v=0$): 72; $b^1\Sigma_g^+$ ($v=2$)$-X^3\Sigma_g^-$ ($v=0$): 49				

[a] These constants were used in the construction [9] of HITRAN parameters for these bands.
[b] The zero point energy is taken where Eq. (1) yields zero (see Fig. 3). The lowest populated energy level of $^{16}O_2$ will be 0.24584 cm^{-1} above this origin.

original publication. Although Ref. [26] provides the spectroscopic constants, it does not give information on how many lines were measured and therefore the range of validity of the reported constants. Moreover, Brown and Plymate [11] found that line positions for the $b^1\Sigma_g^+$ ($v=0$)$-X^3\Sigma_g^-$ ($v=0$) band of oxygen reported by Phillips et al. [26] systematically differ from theirs by about -0.012 cm^{-1}, while the later very high-precision study by Robichaud et al. [27] showed a very good agreement with Ref. [11]. With that in mind, one can assume that adding the line positions from Ref. [26] into the fit would not necessarily improve its quality.

The SPFIT program [28] was used to carry out the global fit. The ground state was fitted to an effective Hamiltonian represented by

$$H_{eff}=B\mathbf{N}^2-D\mathbf{N}^4+H\mathbf{N}^6+\left[\lambda+\lambda_D\mathbf{N}^2+\lambda_H\mathbf{N}^4\right]\tfrac{2}{3}(3S_z^2-\mathbf{S}^2)+[\gamma+\gamma_D\mathbf{N}^2+\gamma_H\mathbf{N}^4]\mathbf{N}\cdot\mathbf{S} \quad (1)$$

where B, λ and γ are rotational, spin–spin, and spin–rotation interaction constants, respectively, while the other constants are their first and second order centrifugal distortion terms. $\mathbf{N}$ represents the rotational angular momentum, and $\mathbf{S}$ and S_z represent total electron spin and its projection onto the internuclear axis (the total angular momentum $\mathbf{J}=\mathbf{N}+\mathbf{S}$ in Hund's case (b)).

The rotational energies in the $a^1\Delta_g$ ($v=0$) and $b^1\Sigma_g^+$ ($v=1$) states were fitted to Eq. (2) (note that Λ-doubling

Author's personal copy

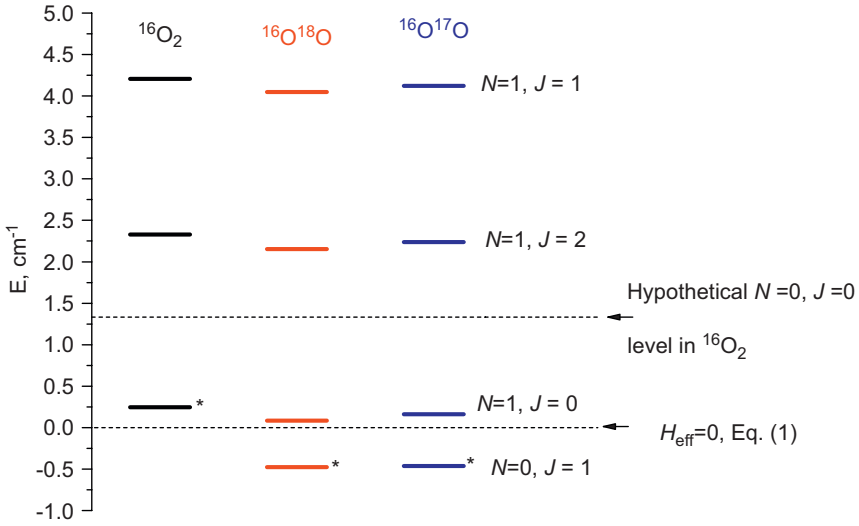

Fig. 3. Lowest energy levels of the isotopologues of oxygen in the ground electronic state and their location with respect to the zero energy, i.e. when H_{eff} in Eq. (1) is equal to zero. The hypothetical $N=0, J=0$ level is also indicated. Asterisks (*) show the lowest populated levels that are often chosen to be a reference zero point energy (such as in HITRAN).

in the $a^1\Delta_g$ ($v=0$) state is not resolved).

$$F(J)=T+BJ(J+1)-D[J(J+1)]^2+H[J(J+1)]^3, \quad (2)$$

where T is an electronic state term value. The resulting spectroscopic constants for the $b^1\Sigma_g^+$ ($v=1$) state are given in Table 1, along with other values reported in the literature. It was found that for the $b^1\Sigma_g^+$ ($v=1$) level, the distortion constant H was largely undetermined; therefore, the corresponding term was removed from the fit of that state. The output files of the SPFIT program can be obtained from the authors on request. It is worth noting that none of the available measurements of the transitions that involve the $b^1\Sigma_g^+$ ($v=1$) state have uncertainties better than 0.002 cm^{-1}, which is an uncertainty given for five lines measured in Ref. [25]. The $b^1\Sigma_g^+$ ($v=1$)–$X^3\Sigma_g^-$ ($v=0$) line positions have uncertainties of 0.01 cm^{-1} while those from the $b^1\Sigma_g^+$ ($v=1$)–$a^1\Delta_g$ ($v=0$) band are 0.005 cm^{-1}. Although, as can be seen from the validation section below, the line positions generated from the constants obtained in the global fit performed here seem to be superior to those from HITRAN that are based on the constants from Ref. [13] obtained through the fit of solar atmospheric spectrum reported by Babcock and Herzberg [14], there is still an obvious need of higher-resolution measurements under controlled laboratory conditions.

Table 1 compares the constants obtained in this work with ones from previous investigations. It is important to mention the long-standing issue of the choice of zero-point energy for calculation of the molecular oxygen electronic-state term values. Zero in this work corresponds to when $H_{eff}=0$ in Eq. (1), but, the zero-point energy is often taken at the level when $N=0$ and $J=0$ in the ground electronic state $X^3\Sigma_g^-$. However, because in oxygen such a level does not exist, many researchers prefer to choose the lowest populated energy level as a zero-point reference. In this way, for the $^{16}O_2$ isotopologue the lowest energy level is $N=1, J=0$, whereas for the $^{16}O^{18}O$ and $^{16}O^{17}O$ isotopologues the lowest energy level is $N=0, J=1$. Fig. 3 shows where the lowest fine structure levels of the oxygen isotopologues are located (on the energy scale) with respect to the hypothetical $N=0, J=0$ level and when expression in Eq. (1) yields zero. In general, either way of choosing the zero-point energy is correct as long as it is clearly stated.

2.1.2. $^{16}O^{18}O$ and $^{16}O^{17}O$

The only available high-resolution study (under controlled laboratory conditions) of the B-band for the $^{16}O^{18}O$ and $^{16}O^{17}O$ isotopologues is that by Naus et al. [30]. The line positions of the $^{16}O^{18}O$ B-band from Naus et al. [30] were fitted in combination with the microwave data taken from the supplementary material of Ref. [20] that contains the measurements carried out in that work and references therein. The results of the fit for this isotopologue are given in Table 2. When one compares the $^{16}O^{18}O$ constants derived in this study with ones from Naus et al. [30] the disagreement in the distortion constants is apparent, while essentially the same data were used in the fit here and in Ref. [30]. The disagreement is merely due to the fact that in the fit in Ref. [30], the ground state constants were fixed to the ones reported by Steinbach and Gordy [31], where the D constant was not determined experimentally but rather calculated from the $^{16}O_2$ D constant using the isotopic relation. Since we have used an extensive (in terms of range of rotational levels) set of microwave transitions from the supplementary material of Ref. [20], it is likely that the distortion constant of the upper state determined here is more accurate than the one reported in Ref. [30].

In the fit of the $^{16}O^{17}O$ isotopologue B-band line positions [30], the ground-state constants were held fixed to the ones reported by Leshchishina et al. [32] that are based on the combined fit of the $a^1\Delta_g$ ($v=0$)–$X^3\Sigma_g^-$ ($v=0$) band and MW data from Cazzoli et al. [33]. The results of the fit for these two isotopologues are given in

Author's personal copy

Table 2
Spectroscopic parameters of the $v=1$ and 2 levels of the $b^1\Sigma_g^+$ state of $^{16}O^{18}O$.

Parameters (cm^{-1})	This work	Babcock and Herzberg [14]	Naus et al. [30]	HITRAN [18]
T_1	14,490.14425(257) [a]	14,488.84	14,490.145(3) [a]	14,488.826
B_1	1.297296(35)	1.29740	1.29727(3)	1.29717
D_1	$4.897(92)\times10^{-6}$		$4.80(8)\times10^{-6}$	4.6
T_2	15,829.5491(207) [a]			15,828.247
B_2	1.28056(36)			1.279
D_2	$5.37(123)\times10^{-6}$			4.86×10^{-6}
Number of lines used in this work per band	MW: 85; $b^1\Sigma_g^+$ ($v=1$)–$X^3\Sigma_g^-$ ($v=0$): 72; $b^1\Sigma_g^+$ ($v=2$)–$X^3\Sigma_g^-$ ($v=0$): 49			

[a] The zero point energy is taken where Eq. (1) yields zero (see Fig. 3). The lowest energy level of $^{16}O^{18}O$ will be 0.47795 cm^{-1} below this origin. The empirical shift of +0.005 cm^{-1} is not included in this term energy value.

Table 3
Spectroscopic parameters of the $v=1$ level of the $b^1\Sigma_g^+$ state of $^{16}O^{17}O$. The ground state constants were fixed to those from Ref. [32]. 98 lines from the B-band were used in the fit.

Parameters (cm^{-1})	This work	Babcock and Herzberg [14]	Naus et al. [29]
T_1	14,507.5841(20) [a]	14,506.26	14,507.583(2) [a]
B_1	1.332774(15)	1.3331	1.332761(15)
D_1	$5.031(21)\times10^{-6}$		$5.11(2)\times10^{-6}$

[a] The zero point energy is taken for when Eq. (1) yields zero (see Fig. 3). The lowest energy level of $^{16}O^{17}O$ will be 0.46452 cm^{-1} below this origin.

Table 3. Similarly to the case of $^{16}O^{18}O$, when one compares the $^{16}O^{17}O$ constants derived in this study with ones from Naus et al. [30], the disagreement in the distortion constants is noticeable, while essentially the same data were used in the fit here and in Ref. [30]. In this case in the fit in Ref. [30], the ground-state constants were fixed to the ones reported by Cazzoli et al. [33], where the D constants were also not determined experimentally but derived from the $^{16}O_2$ constants. It is therefore also likely that the distortion constant determined here is more accurate.

The constants from Tables 2 and 3 were used to generate the line positions, which were tested against the solar atmospheric spectrum. While line positions generated by such a method for the $^{16}O^{17}O$ species appear to be satisfactory, the line positions for $^{16}O^{18}O$ seem to be systematically shifted by +0.005 cm^{-1}. It is hard to explain such a discrepancy. Experiments of Naus et al. [30] were carried out at 30 Torr, which could result in a pressure shift of only about 0.0012 cm^{-1}. Note that retrievals in Fig. 1b were carried out with the inclusion of the line shifts (see corresponding section for details). In the final line list, it was decided to add 0.005 cm^{-1} to the value of the $^{16}O^{18}O$ band origin given in Table 1. Additional experiments are needed to address this problem.

2.2. Intensities

As pointed out by Long et al. [34], HITRAN line intensities in the A-band (and other HITRAN oxygen bands that involve the $b^1\Sigma_g^+$ state) contain an error associated with the wrong coding of intensity calculations inherited from Ref. [9]. In order to remove this error, line intensities need to be multiplied by a factor $(\nu_{line}/\nu_{band})^3$, which results in a reduction of the intensities for the P-branches and an increase in the R-branches. Here, ν_{line} is the line position of the transition and ν_{band} is the band origin. In addition, we introduced an additional scaling factor of 1.02 to better match the results of high-precision measurements by Lisak et al. [25]. There are still some rotationally dependent discrepancies that exist even after the aforementioned corrections. These discrepancies occur due to the necessity of inclusion of the ro-vibronic Frank–Condon factors, instead of using just the vibronic Frank–Condon factor that is being absorbed into the integrated band intensity value used as an input in the program associated with Ref. [9]. The calculation of these factors can potentially be carried out using potential energy functions inputted into a program such as Le Roy's program LEVEL ⟨http://scienide2.uwaterloo.ca/~rleroy/level/⟩.

For the $^{16}O^{18}O$ and $^{16}O^{17}O$ isotopologues, intensities calculated for the principal isotopologue were simply scaled by the isotopic abundance. This is, of course, a crude method since the Frank–Condon factors should be different in different isotopologues. In fact, while this procedure seems to work well in application to the $^{16}O^{18}O$ species when compared to the solar atmospheric spectrum, the intensities of $^{16}O^{17}O$ appear to be underestimated by a factor of approximately 1.5. This additional empirical factor was therefore introduced for the $^{16}O^{17}O$ species. In the end, effectively the new $^{16}O^{17}O$ intensities in the B-band differ from those in HITRAN2008 by different factors, and in some extreme cases are 10 times weaker. Note, that contrary to our assertion, Motto-Ros et al. [35] had suggested that $^{16}O^{17}O$ lines in HITRAN had underestimated (by about 40%) rather than overestimated intensity. They tried to explain the discrepancy in intensity and air-broadening (which will be discussed further) with the following sentence: "*This can be explained by the fact that* ab initio *calculations of parameters of weak*

Author's personal copy

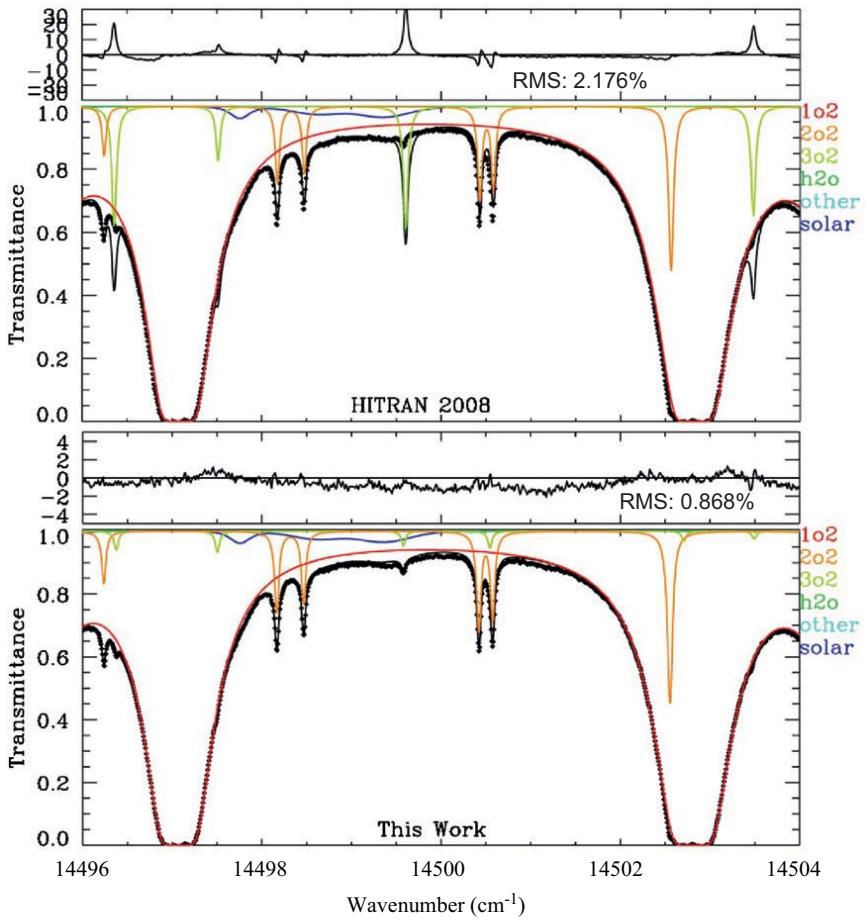

Fig. 4. The 14,496–14,504 cm^{-1} region in the B-band, which contains the strongest lines of the $^{16}O^{17}O$ isotopologue (3o2: lime green curves). The top panel shows the fit using HITRAN 2008 while the bottom panel employs the new line list. (For interpretation of the references to color in this figure legend, the reader is referred to the web version of this article.)

transitions are difficult and cannot achieve sufficient accuracy". This sentence has no valid basis as HITRAN parameters were not based on the ab initio calculations. It is hard to explain the discrepancy between our finding and that of Motto-Ros et al. [35], but the fact that HITRAN intensities for $^{16}O^{17}O$ lines were overestimated can be clearly seen in top panel of Fig. 4. Fig. 4 zooms into the 14,496–14,504 cm^{-1} region, which contains the strongest lines of the $^{16}O^{17}O$ isotopologue (3o2: lime green curves). The HITRAN 2008 line list overestimates the intensities of these particular lines by factors of up to 10, resulting in large positive residuals in the simulated spectrum (top panel). The bottom panel of Fig. 4 shows the improvement of the residuals with the new parameters derived here.

2.3. Self-broadened half widths

Self-broadened half widths, γ_{self}, in the B-band have been measured in the works of Barnes and Hays [15] and Lisak et al. [25] up to $J'=26$, where J' is the quanta of rotational angular momentum in the upper state. These measurements are shown in Fig. 5. When assessing functional dependence of measured broadening coefficients in the A-band, Yang et al. [36] have found that the following function of upper state J-level (J') fits data the best while having good predictive abilities:

$$\gamma = A + \frac{B}{1 + c_1 J' + c_2 J'^2 + c_3 J'^4}. \quad (3)$$

This expression has been adapted for the other recent works devoted to the A-band, for example Refs. [34,37]. The relatively short extent of the available experimental data for the B-band unfortunately does not allow fitting them efficiently to Eq. (3) without fixing some of the constants to the guessed values. Meanwhile, if one uses Eq. (3) with coefficients derived in the A-band studies in either Refs. [34] or [37] it is clear that they can be applied to simulate the data in the B-band in particular with coefficients from Long et al. [34]. In the construction of the new line list, these coefficients were applied to all three oxygen isotopologues in HITRAN, because of the weak isotopic dependence of self-broadened half widths in molecular oxygen.

2.4. Air-broadened half widths

Air-broadened Lorentzian half widths in the B-band that were measured in the works of Barnes and Hays [15] ($J' \leq 18$)

Author's personal copy

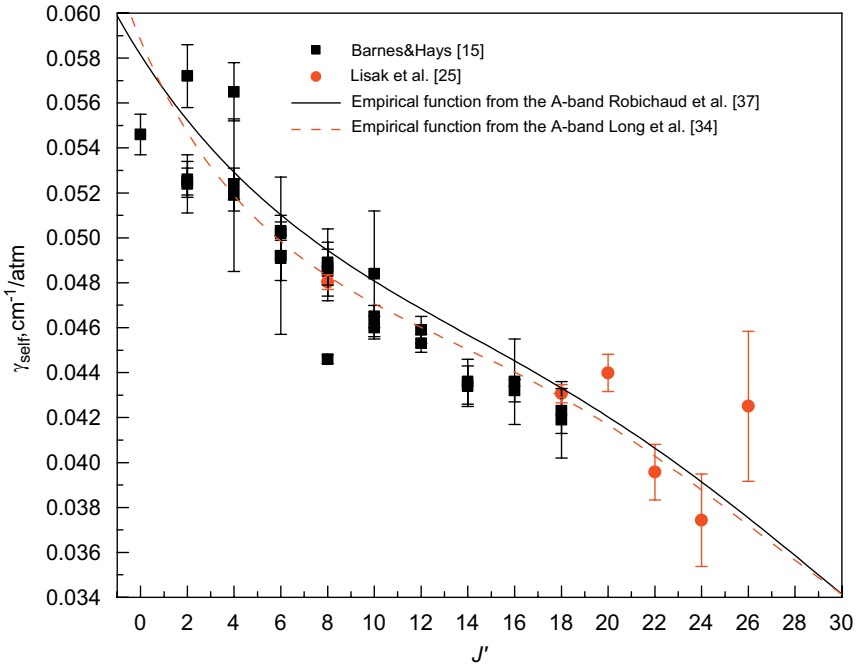

Fig. 5. Self-broadened half widths in the B-band (see text for details).

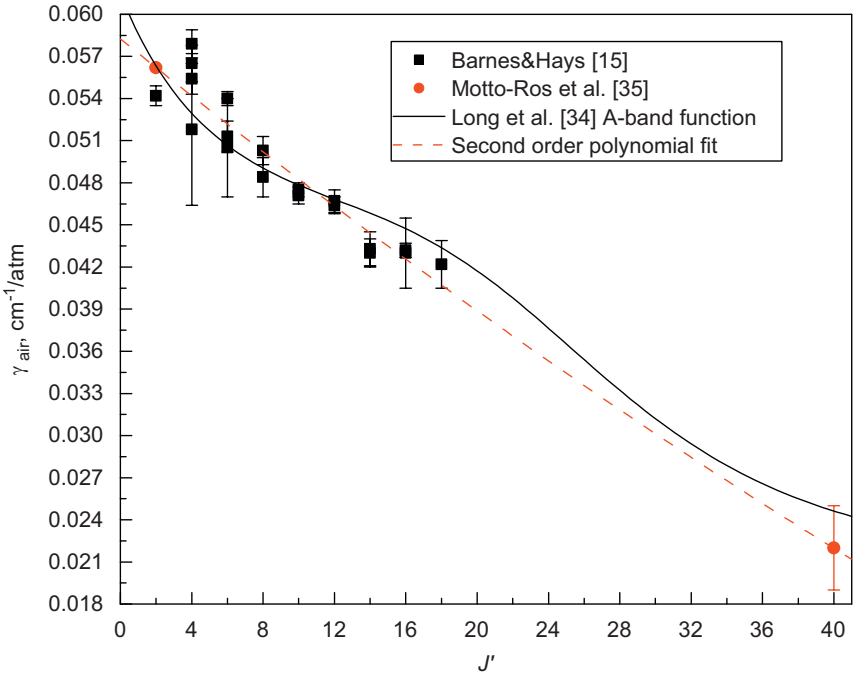

Fig. 6. Air-broadened half widths in the B-band (see text for details).

and Motto-Ros et al. [35] ($J'=2$ and 40) are shown in Fig. 6 with their experimental uncertainties. The curve corresponding to Eq. (3) with A-band-derived coefficients from Long et al. [34] (same as in Robichaud et al. [37]) is also shown in that figure. Just like in the case of self-broadening, the A-band-derived function reproduces the measurements in the B-band predominantly within experimental uncertainty. We also note that the experimental data fit well ($R^2=0.97$) to just a second order polynomial

$$\gamma_{air} = 0.05826(16) - 0.00103(5)J' + 3.1(21) \times 10^{-6} J'^2. \quad (4)$$

The numbers in parentheses are one standard deviation in the units of the last digit. This polynomial was used in the construction of the new B-band line list up to

Author's personal copy

$J'=40$, and the value of $\gamma_{air}=0.0220\ cm^{-1}$/atm was assigned to all lines with $J'>40$. This algorithm was used for all HITRAN isotopologues of molecular oxygen in the B-band. Note, however, that Motto-Ros et al. [35] have determined that air broadening of the R11Q12 and R13R13 lines of the $^{16}O^{17}O$ species is significantly (over 40%) larger than those given in HITRAN2004 (which were the same as for the $^{16}O_2$ species, and for these two lines are not very different from the ones determined in this work). The "ab initio" arguments in Ref. [35] regarding discrepancies in their measurements of $^{16}O^{17}O$ intensities and air-broadening coefficients had been addressed in the previous section on intensity, and, as mentioned, it does not have a valid foundation. The anomalous broadening of the $^{16}O^{17}O$ species reported in Ref. [35] may be partially attributed to the hyperfine splitting in the ground electronic state, which is found to be pronounced in the A-band [38].

2.5. Pressure shift (air)

Since pressure shifts in molecular oxygen do not have strong isotopic dependence, we used one algorithm for all three species. Pressure shifts of the $b^1\Sigma_g^+-X^3\Sigma_g^-$ band cannot be modeled with simple polynomial approximations as functions of upper state rotational quantum number; therefore, a different approach was chosen.

Pressure (air)-shifting coefficients from the experimental work of Barnes and Hays [15] were used when available. In case the measurements were not available, empirically scaled line shifts from the A-band in HITRAN2008 were used. These A-band values are based on the measurements by Robichaud et al. [27] for the P-lines, while the average of experimental values reported by Predoi-Cross et al. [39,40] were used for R-lines. We used an empirical scaling coefficient of 1.22. Fig. 7 shows how the scaled A-band values compare with the B-band measurements by Barnes and Hays [15].

3. γ-Band

3.1. Line positions

As mentioned above, the line positions for the γ-band in the HITRAN database are based on the constants derived from the reanalysis of the Babcock and Hertzberg solar atmospheric spectra [14] by Albritton et al. [13]. Two independent high-resolution laboratory studies of the line positions in the γ-band have been carried out since then by Naus et al. [29] using CRDS technique and by Cheah et al. [24] using FTS. These measurements in general agree with each other within experimental uncertainty, which appears to be around $0.01\ cm^{-1}$ in both works. After carrying out independent and combined fits of these two datasets in combination with all the data used to fit $^{16}O_2$ spectra in the B-band, it appears that the band origin obtained from the fit of just Naus et al. [29] data agrees a little better with our atmospheric spectrum than the one obtained from the fit of Cheah et al. [24] or combined data (the difference is about $0.007\ cm^{-1}$). Hence, for the current effort, the parameters have been obtained from the fit of only Naus et al. [29] data. The $b^1\Sigma_g^+$ ($v=2$) spectroscopic constants obtained from this fit are given in Table 1. There is, however, an obvious need of new independent measurements of the line positions in the γ-band.

Unfortunately there are still no laboratory measurements available for the $^{16}O^{18}O$ lines in this band. Ironically, although this isotopologue is the second most

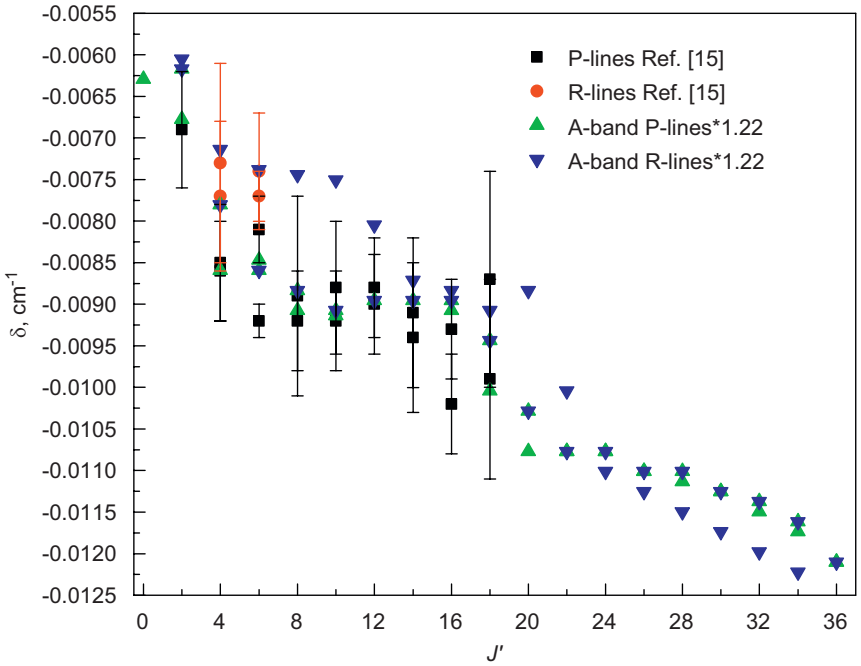

Fig. 7. Pressure shifts (δ) in the B-band (see text for details).

Author's personal copy

abundant in the atmosphere, it is the only one for which no measurements are available while $^{16}O_2$, $^{16}O^{17}O$, $^{17}O_2$, and $^{18}O_2$ were measured in Ref. [29].

It was, therefore, decided to assign and fit the $^{16}O^{18}O$ features in the Kitt Peak atmospheric spectrum. In total, 23 $^{16}O^{18}O$ γ-band lines were assigned with the uncertainty ranging from 0.03 to 0.05 cm^{-1} (lines are given in the Supplementary material). They were fit together with all the same data for these species that were used in the fit of the B-band. The resulting $^{16}O^{18}O$ γ-band constants are given in Table 2.

3.2. Intensities

From our analyses of the Kitt Peak atmospheric spectra, the HITRAN 2008 intensities in the γ-band appear to be underestimated by approximately 20%. These intensities are based on the work by Mélières et al. [17]. Interestingly, the earlier work by Miller et al. [41] reported an integrated band strength almost exactly 20% higher than that reported in Ref. [17]. Therefore, it was decided to use the results from Miller et al. [41] for the new line list.

3.3. Self-broadened half widths

Self-broadened half widths in the γ-band have been measured in the works of Barnes and Hays [15] and Mélières et al. [17] up to $J'=26$, and these measurements are shown in Fig. 8. Just as in the case of the B-band, it is clear that Eq. (3) with coefficients derived from either Refs. [34] or [37] can be used efficiently in application to the γ-band. In this case, however, the use of coefficients from Robichaud et al. [37] seem to provide better agreement with the direct γ-band measurements. In Fig. 7 we also demonstrate that the use of Eq. (3) with A-band-derived coefficients is more efficient for predictive purposes than polynomials that are fitted directly to the γ-band measurements themselves. Fig. 8 demonstrates that using Eq. (3) with the A-band coefficients clearly reproduces a data better than the third order polynomial fit.

3.4. Air-broadened half widths

Air-broadened half widths measured by Barnes and Hays [15] and Mélières et al. [17] are shown in Fig. 9. The empirical function, Eq. (3), derived from the A-band measurements (Long et al. [34] and Robichaud et al. [37]) is also shown in the figure. One can see that unlike the case of the B-band, the A-band-derived function underestimates the air-broadening values in the γ-band. Therefore, in this effort this function was empirically adjusted by setting the A and B coefficients (see Eq. (3)) to be equal to 0.02197 and 0.04113 cm^{-1}/atm, respectively. The c_1, c_2 and c_3 coefficients remained unchanged.

3.5. Pressure shift (air)

The approach used for assigning values of pressure shifts to all transitions in the γ-band was same as the one used for the B-band.

Pressure (air)-shifting coefficients from the experimental work of Barnes and Hays [15] were used when available. In case the measurements were not available, empirically scaled line shifts from the A-band in HITRAN2008 were used. We used an empirical scaling coefficient of 1.36. Fig. 10 shows how the scaled A-band

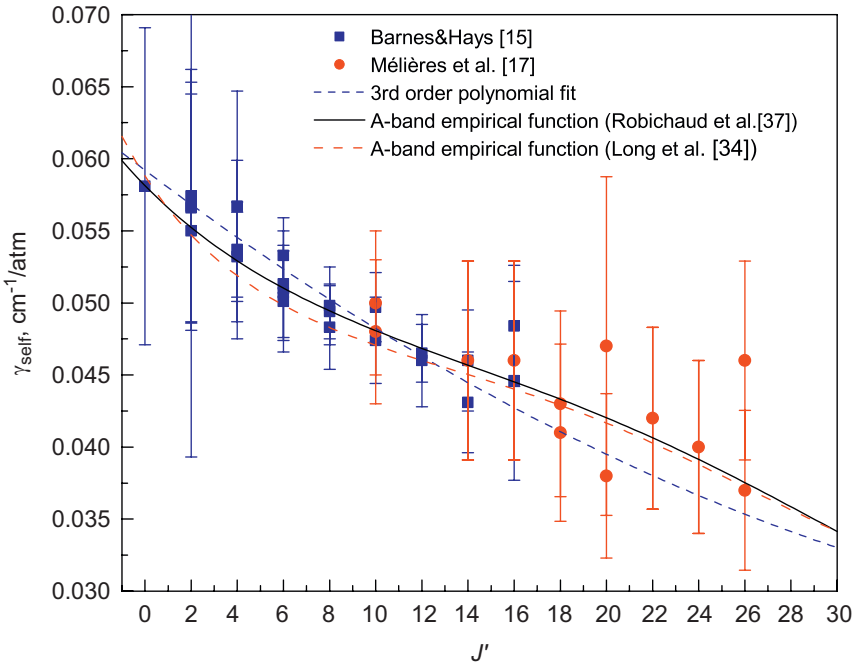

Fig. 8. Self-broadened half widths in the γ-band (see text for details).

Author's personal copy

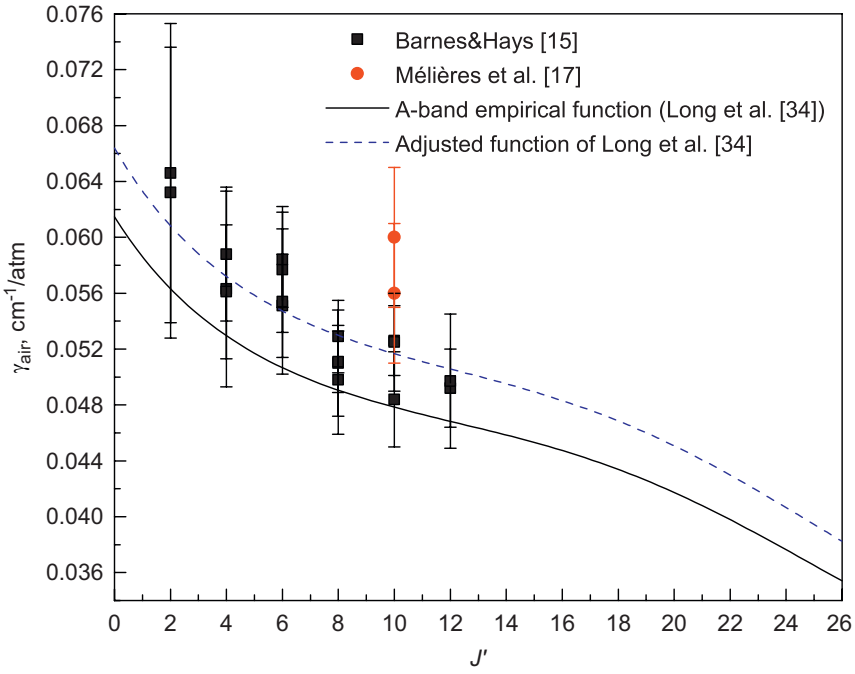

Fig. 9. Air-broadened half widths in the γ-band (see text for details).

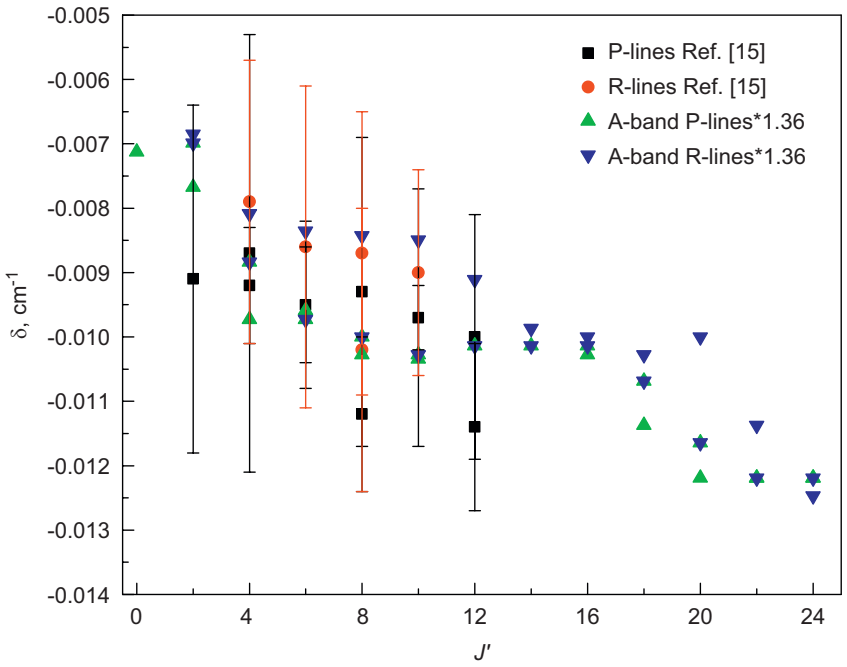

Fig. 10. Pressure shifts (δ) in the γ-band (see text for details).

values compare with the γ-band measurements by Barnes and Hays [15].

4. Validation of the new line list

The new line lists that are described in this paper have been validated against Park Falls and Kitt Peak spectra. As one can see in the bottom panel of Fig. 1 the new line list for the B-band results in a dramatic improvement in the quality of the spectral fits, with the overall spectral residual dropping by over a factor two, from 2.18% (when using HITRAN 2008) to 0.868% rms.

In panel (c) of Fig. 2 the residuals in the γ-band improved to 0.527% rms, mainly as a result of the

Author's personal copy

Table 4
O_2 scale factors derived from fitting atmospheric spectra.

	Isotopologue	HITRAN 08	This Work
B-band	$^{16}O_2$	1.025 ± 0.02	1.005 ± 0.01
	$^{16}O^{18}O$	1.04 ± 0.03	1.02 ± 0.02
	$^{16}O^{17}O$	0.30 ± 0.1	0.99 ± 0.05
γ-band	$^{16}O_2$	1.20 ± 0.02	1.00 ± 0.02
	$^{16}O^{18}O$	1.3 ± 0.5	1.1 ± 0.2

substantially improved line positions and intensities and the addition of 66 missing $^{16}O^{18}O$ lines.

Most of the remaining residuals in both figures are due to other sources of inaccuracies, such as contributions from other species and solar lines, as well as the presence of line mixing that is especially pronounced in the band heads of both bands and has not been modeled here. Table 4 shows the average ratio between the retrieved atmospheric O_2 column amounts, and those expected from the known atmospheric path and O_2 mole fraction. Values greater than unity imply that the line intensities have to be increased, and vice versa. There is an obvious improvement in our work. The remaining differences are within experimental uncertainty and should be addressed via additional experiments.

The spectroscopic constants derived in this work for the $b^1\Sigma_g^+$ ($v=1$) state were also used for recalculation of line positions in the $b^1\Sigma_g^+$ ($v=1$)$-X^3\Sigma_g^-$ ($v=1$) band at 0.77 μm (the A-band hot band). The new parameters were tested against TCCON and Kitt Peak solar atmospheric spectra and yielded slightly improved spectral fits in comparison with the HITRAN2008 parameters. The new line list for the $b^1\Sigma_g^+$ ($v=1$)$-X^3\Sigma_g^-$ ($v=1$) band is also given in the Supplementary material.

5. Conclusion

A careful review of the available line position, intensity and line-shape measurements in the B and γ-bands of oxygen was carried out and new spectral parameters were derived based on that review. These parameters were used to generate a new reference spectroscopic line list that will be included in the future edition of the HITRAN database. The new parameters have been validated against atmospheric spectra recorded with solar-pointing Fourier transform spectrometers in Park Falls and Kitt Peak. The use of the new parameters yielded pronounced improvements in the residuals in comparison with those obtained using the current edition of the HITRAN database [18]. Atmospheric spectra from solar pointing FTS prove to be an excellent tool for validation of oxygen spectral parameters as demonstrated in Ref. [42] and in this work.

Although the line parameters reported here are unambiguously improved with respect to previous versions of the HITRAN database, there is still a lot of room for improvement concerning the measurements of line positions and pressure shifts. Additional high-resolution, high-accuracy experiments are needed.

In the future, it would also be worthwhile to add the $^{16}O^{17}O$ isotopologue in the γ-band. In addition, the $b^1\Sigma_g^+$ (v=3)$-X^3\Sigma_g^-$ ($v=0$) band near 17,200 cm^{-1} has absorption lines that are up to 20% deep in high-air-mass ground-based spectra, and therefore should be considered for inclusion in HITRAN. Interestingly, available high-resolution measurements of this band by Naus and Ubachs [43] and Biennier and Campargue [44] do not agree very well with each other in line positions (an average discrepancy of 0.012 cm^{-1}) and in integrated intensities (disagreeing by almost 40%). It will be interesting to validate these data versus ground-based atmospheric spectra.

Acknowledgments

We would like to thank Joseph Hodges and Daniel Lisak for providing us with unpublished line position measurements of five transitions in the B-band. Helpful discussions with Linda Brown and Caroline Nowlan are much appreciated. The work carried out at the Harvard-Smithsonian Center for Astrophysics was supported by NASA through the Earth Observing System (EOS) under grant NAG5-13534. Part of this work was performed at the Jet Propulsion Laboratory, California Institute of Technology, under contract with NASA. We thank the Kitt Peak National Observatory, and the Total Column Carbon Observing Network (TCCON) for providing the atmospheric spectra used to validate the new line lists.

Appendix A. Supplementary material

Supplementary data associated with this article can be found in the online version at doi:10.1016/j.jqsrt.2011.05.007.

References

[1] Crisp D, Atlas RM, Breon FM, Brown LR, Burrows JP, Ciais P, et al. The orbiting carbon observatory (OCO) mission. Adv Space Res 2004;34:700–9.
[2] Yokomizo M. Greenhouse gases observing satellite (GOSAT) ground systems. Fujitsu Sci Tech J 2008;44:410–7.
[3] Bovensmann H, Burrows JP, Buchwitz M, Frerick J, Noel S, Rozanov VV, et al. SCIAMACHY: Mission objectives and measurement modes. Am Meteorol Soc 1999:127–50.
[4] Nowlan CR, McElroy CT, Drummond JR. Measurements of the O_2 A- and B-bands for determining temperature and pressure profiles from ACE-MAESTRO: Forward model and retrieval algorithm. J Quant Spectrosc Radiat Transfer 2007;108:371–88.
[5] Frankenberg C, Butz A, Toon GC. Disentangling chlorophyll fluorescence from atmospheric scattering effects in O_2 A-band spectra of reflected sun-light. Geophys Res Lett 2011;38:03801.
[6] Kuze A, Chance KV. Analysis of cloud top height and cloud coverage from satellites using the O_2 A and B bands. J Geophys Res 1994;99:14481–91.
[7] Daniel JS, Solomon S, Miller HL, Langford AO, Portmann RW, Eubank CS. Retrieving cloud information from passive measurements of solar radiation absorbed by molecular oxygen and O_2-O_2. J Geophys Res 2003;108:4515.
[8] Ortland DA, Skinner WR, Hays PB, Burrage MD, Lieberman RS, Marshall AR, et al. Measurements of stratospheric winds by the high resolution Doppler imager. J Geophys Res 1996;101:10351–63.
[9] Gamache RR, Goldman A, Rothman LS. Improved spectral parameters for the three most abundant isotopomers of the oxygen molecule. J Quant Spectrosc Radiat Transfer 1998;59:495–509.
[10] Rothman LS, Jacquemart D, Barbe A, Chris Benner D, Birk M, Brown LR, et al. The HITRAN 2004 molecular spectroscopic database. J Quant Spectrosc Radiat Transfer 2005;96:139–204.
[11] Brown LR, Plymate C. Experimental line parameters of the oxygen A Band at 760 nm. J Mol Spectrosc 2000;199:166–79.

Author's personal copy

[12] Rouillé G, Millot G, Saint-Loup R, Berger H. High-resolution stimulated Raman spectroscopy of O_2. J Mol Spectrosc 1992;154:372–82.

[13] Albritton DL, Harrop WJ, Schmeltekopf AL, Zare RN. Resolution of the discrepancies concerning the optical and microwave values for B_0 and D_0 of the $X^3\Sigma_g^-$ state of O_2. J Mol Spectrosc 1973;46:103–18.

[14] Babcock HD, Herzberg L. Fine structure of the red system of atmospheric oxygen bands. Astrophys J 1948;108:167–90.

[15] Barnes JE, Hays PB. Pressure shifts and pressure broadening of the B and γ bands of oxygen. J Mol Spectrosc 2002;216:98–104.

[16] Giver LP, Boese RW, Miller JH. Intensity measurements, self-broadening coefficients, and rotational intensity distribution for lines of the oxygen B band at 6880 Å. J Quant Spectrosc Radiat Transfer 1974;14:793–802.

[17] Mélières MA, Chenevier M, Stoeckel F. Intensity measurements and self-broadening coefficients in the γ band of O_2 at 628 nm using intracavity laser-absorption spectroscopy (ICLAS). J Quant Spectrosc Radiat Transfer 1985;33:337–45.

[18] Rothman LS, Gordon IE, Barbe A, Benner DC, Bernath PF, Birk M, et al. The HITRAN 2008 molecular spectroscopic database. J Quant Spectrosc Radiat Transfer 2009;110:533–72.

[19] Rothman LS, Rinsland CP, Goldman A, Massie ST, Edwards DP, Flaud JM, et al. The HITRAN molecular spectroscopic database and HAWKS (HITRAN atmospheric workstation): 1996 edition. J Quant Spectrosc Radiat Transfer 1998;60:665–710.

[20] Drouin BJ, Yu S, Miller CE, Müller HSP, Lewen F, Brünken S, et al. Terahertz spectroscopy of oxygen, O_2, in its $^3\Sigma$ and $^1\Delta$ electronic states: THz Spectroscopy of O_2. J Quant Spectrosc Radiat Transfer 2010;111:1167–73.

[21] Millot G, Lavorel B, Fanjoux G. Pressure broadening, shift, and interference effect for a multiplet line in the rovibrational anisotropic stimulated Raman spectrum of molecular oxygen. J Mol Spectrosc 1996;176:211–8.

[22] Foldes T, Cermak P, Macko M, Veis P, Macko P. Cavity ring-down spectroscopy of singlet oxygen generated in microwave plasma. Chem Phys Lett 2009;467:233–6.

[23] Leshchishina O, Kassi S, Gordon IE, Rothman LS, Wang L, Campargue A. High sensitivity CRDS of the $a^1\Delta_g - X^3\Sigma_g^-$ band of oxygen near 1.27 μm: extended observations, quadrupole transitions, hot bands and minor isotopologues. J Quant Spectrosc Radiat Transfer 2010;111:2236–45.

[24] Cheah S-L, Lee Y-P, Ogilvie JF. Wavenumbers, strengths, widths and shifts with pressure of lines in four bands of gaseous $^{16}O_2$ in the systems $a^1\Delta_g - X^3\Sigma_g^-$ and $b^1\Sigma_g^+ - X^3\Sigma_g^-$. J Quant Spectrosc Radiat Transfer 2000;64:467–82.

[25] Lisak D, Masłowski P, Cygan A, Bielska K, Wójtewicz S, Piwiński M, et al. Line shapes and intensities of self-broadened O_2 $b^1\Sigma_g^+$ $(v=1) - X^3\Sigma_g^-(v=0)$ band transitions measured by cavity ring-down spectroscopy. Phys Rev A 2010;81:42504.

[26] Phillips AJ, Peters F, Hamilton PA. Precision emission and absorption spectroscopy of the oxygen atmospheric bands ($b^1\Sigma_g^+ - X^3\Sigma_g^-$) from Fourier transform spectroscopy. J Mol Spectrosc 1997;184:162–6.

[27] Robichaud DJ, Hodges JT, Maslowski P, Yeung LY, Okumura M, Miller CE, et al. High-accuracy transition frequencies for the O_2 A-band. J Mol Spectrosc 2008;251:27–37.

[28] Pickett HM. The fitting and prediction of vibration-rotation spectra with spin interactions. J Mol Spectrosc 1991;148:371–7.

[29] Naus H, Navaian K, Ubachs W. The γ-band of $^{16}O_2$, $^{16}O^{17}O$, $^{17}O_2$ and $^{18}O_2$. Spectrochim Acta Part A: Mol Biomol Spectrosc 1999;55: 1255–62.

[30] Naus H, van der Wiel SJ, Ubachs W. Cavity-ring-down spectroscopy on the $b^1\Sigma_g^+ - X^3\Sigma_g^-(1,0)$ band of oxygen isotopomers. J Mol Spectrosc 1998;192:162–8.

[31] Steinbach W, Gordy W. Microwave spectrum and molecular constants of $^{16}O^{18}O$. Phys Rev A 1975;11:729–31.

[32] Leshchishina O, Kassi S, Gordon IE, Yu S, Campargue A. The $a^1\Delta_g - X^3\Sigma_g^-$ band of $^{16}O^{17}O$, $^{17}O^{18}O$ and $^{17}O_2$ by high sensitivity CRDS near 1.27 μm. J Quant Spectrosc Radiat Transfer 2011;112: 1257–65.

[33] Cazzoli G, Degli Esposti C, Favero PG, Severi G. Microwave spectra of $^{16}O^{17}O$ and $^{18}O^{17}O$. Nuovo Cimento B 1981;62:243–54.

[34] Long DA, Havey DK, Okumura M, Miller CE, Hodges JT. O_2 A-band line parameters to support atmospheric remote sensing. J Quant Spectrosc Radiat Transfer 2010;111:2021–36.

[35] Motto-Ros V, Durand M, Morville J. Extensive characterization of the optical feedback cavity enhanced absorption spectroscopy (OF-CEAS) technique: ringdown-time calibration of the absorption scale. Appl Phys B: Lasers Opt 2008;91:203–11.

[36] Yang Z, Wennberg PO, Cageao RP, Pongetti TJ, Toon GC, Sander SP. Ground-based photon path measurements from solar absorption spectra of the O_2 A-band. J Quant Spectrosc Radiat Transfer 2005;90:309–21.

[37] Robichaud DJ, Hodges JT, Brown LR, Lisak D, Maslowski P, Yeung LY, et al. Experimental intensity and lineshape parameters of the oxygen A-band using frequency-stabilized cavity ring-down spectroscopy. J Mol Spectrosc 2008;248:1–13.

[38] Long DA, Havey DK, Okumura M, Miller CE, Hodges JT. Cavity ring-down spectroscopy measurements of sub-Doppler hyperfine structure. Phys Rev A 2010;81:064502.

[39] Predoi-Cross A, Hambrook K, Keller R, Povey C, Schofield I, Hurtmans D, et al. Spectroscopic lineshape study of the self-perturbed oxygen A-band. J Mol Spectrosc 2008;248:85–110.

[40] Predoi-Cross A, Holladay C, Heung H, Bouanich J-P, Mellau GC, Keller R, et al. Nitrogen-broadened lineshapes in the oxygen A-band: experimental results and theoretical calculations. J Mol Spectrosc 2008;251:159–75.

[41] Miller JH, Giver LP, Boese RW. Intensity measurements for the (2, 0) γ-band of O_2, $b^1\Sigma_g^+ - X^3\Sigma_g^-$. J Quant Spectrosc Radiat Transfer 1976;16:595–8.

[42] Gordon IE, Kassi S, Campargue A, Toon GC. First identification of the $a^1\Delta_g$ - $X^3\Sigma_g^-$ electric quadrupole transitions of oxygen in solar and laboratory spectra. J Quant Spectrosc Radiat Transfer 2010;111: 1174–83.

[43] Naus H, Ubachs W. The $b^1\Sigma_g^+ - X^3\Sigma_g^-$ (3, 0) Band of $^{16}O_2$ and $^{18}O_2$. J Mol Spectrosc 1999;193:442–5.

[44] Biennier L, Campargue A. High resolution spectrum of the (3-0) band of the $b^1\Sigma_g^+ - X^3\Sigma_g^-$ red atmospheric system of oxygen. J Mol Spectrosc 1998;188:248–50.